LAWRENCE
LIVERMORE
NATIONAL
LABORATORY

UCRL-JRNL-212421

Liner Compression of a MAGO / Inverse-Pinch Configuration

R. E. Siemon, W. L. Atchison, T. Awe, B. S. Bauer, A. M. Buyko, V. K. Chernyshev, T. E. Cowan, J. H. Degnan, R. J. Faehl, S. Fuelling, S. F. Garanin, T. Goodrich, A. V. Ivanovsky, I. R. Lindemuth, V. Makhin, V. N. Mokhov, R. E. Reinovsky, D. D. Ryutov, D. W. Scudder, T. Taylor, V. B. Yakubov

May 19, 2005

Nuclear Fusion

Liner compression of a MAGO / inverse-pinch configuration

R.E. Siemon 1), W.L. Atchison 2), T. Awe 1), B.S. Bauer 1), A.M. Buyko 3), V.K. Chernyshev 3), T.E. Cowan 1), J.H. Degnan 4), R.J. Faehl 2), S. Fuelling 1), S.F. Garanin 3), T. Goodrich 1), A.V. Ivanovsky 3), I.R. Lindemuth 1), V. Makhin 1), V.N. Mokhov 3), R.E. Reinovsky 2), D.D. Ryutov 5), D.W. Scudder 2), T. Taylor 2), V.B. Yakubov 3)

1) University of Nevada, Reno; Reno, NV, USA 89557
2) Los Alamos National Laboratory; Los Alamos, NM, USA 87545
3) All-Russian Scientific Research Institute of Experimental Physics (VNIIEF); Sarov, Russia
4) Air Force Research Laboratory; Albuquerque, NM, USA 87117
5) Lawrence Livermore National Laboratory; Livermore, CA, USA 92001

E-mail contact of main author: siemon@unr.edu

Abstract. In the “metal liner” approach to Magnetized Target Fusion (MTF), a preheated magnetized plasma target is compressed to thermonuclear temperature and high density by externally driving the implosion of a flux conserving metal enclosure, or liner, which contains the plasma target. As in inertial confinement fusion, the principle fusion fuel heating mechanism is pdV work by the imploding enclosure, called a pusher in ICF. One possible MTF target, the hard-core diffuse z pinch, has been studied in MAGO experiments at VNIIEF, and is one possible target being considered for experiments on the Atlas pulsed power facility. Numerical MHD simulations show two intriguing and helpful features of the diffuse z pinch with respect to compressional heating. First, in two-dimensional simulations the m=0 interchange modes, arising from an unstable pressure profile, result in turbulent motions and self-organization into a stable pressure profile. The turbulence also gives rise to convective thermal transport, but the level of turbulence saturates at a finite level, and simulations show substantial heating during liner compression despite the turbulence. The second helpful feature is that pressure profile evolution during compression tends towards improved stability rather than instability when analyzed according to the Kadomtsev criteria. A liner experiment is planned for Atlas to study compression of magnetic flux without plasma as a first step. The Atlas geometry is compatible with a diffuse z pinch, and simulations of possible future experiments show that keV temperatures and useful neutron production for diagnostic purposes should be possible if a suitable plasma injector is added to the Atlas facility.

1. Magnetized Target Fusion with a hard-core diffuse z pinch

A plasma target under consideration for application to Magnetized Target Fusion (MTF) (see *e.g.*, [1,2,3] and references therein) is the hard-core diffuse z pinch. The magnetic topology of the configuration is shown in Fig. 1. This configuration occurs in various types of coaxial accelerators such as the MAGO experiments [4,5], or in an inverse pinch geometry [6,7]. In recent simulations [1], the intriguing feature by which a diffuse z pinch self-organizes into a stable pressure profile appears to be a robust process, which is consistent with MAGO experimental results [4]. This paper discusses how the hard core z pinch responds to ideal adiabatic compression, and through numerical modeling what might be expected under more realistic circumstances with heat losses. The results show that thermonuclear temperatures should be achievable by means of plasma compression using liner technology such as that being developed for Explosive Magnetic Generators [8] and the new Atlas pulsed power facility [9]. As an example, parameters are selected for modeling that correspond to a low-cost experiment that might be done on the Atlas facility.

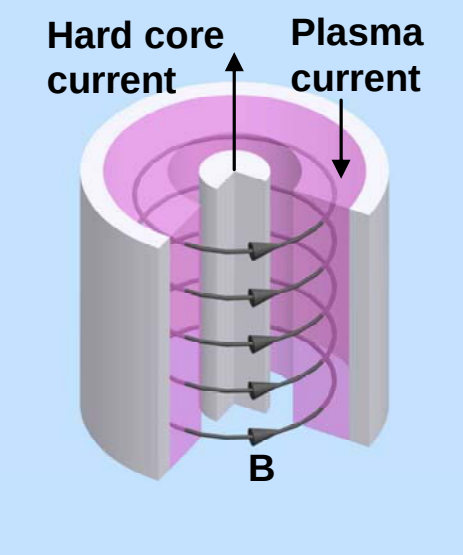

FIG. 1. Magnetic field in the hard-core stabilized diffuse z pinch.

2. Formation, equilibrium, and self-organized stability

As reported at the last IAEA meeting [2], simulations of target plasma formation in an inverse pinch show $m = 0$ instabilities. During the dynamics of formation, plasma acceleration in the radial direction causes Rayleigh-Taylor and Richtmeyer-Meshkov instabilities [7]. As plasma approaches pressure balance between jxB and ∇p, there are also curvature-driven $m = 0$ instabilities as described by Kadomtsev [10]. An intriguing feature is that initially unstable pressure profiles self-organize by means of $m = 0$ interchange motions into stable pressure profiles in the following sense. When fluctuating plasma quantities are averaged along the z direction, the radial profiles of average current and average pressure settle into a one-dimensional equilibrium with finite fluctuations in time and space about equilibrium [1]. The averaged pressure profile becomes stable when examined with respect to the Kadomtsev $m = 0$ criterion for pressure gradient. The $m = 0$ stability criterion can be stated as $Q_0 < 1$, where Q_0 is defined (gas parameter $\gamma = 5/3$):

$$Q_0 = \frac{-(6+5\beta)}{20}\frac{r}{p}\frac{dp}{dr} \qquad (1)$$

In simulations, the kinetic energy associated with instability and turbulent $m = 0$ motion grows exponentially at first, but then saturates as Kadomtsev stable profiles are obtained. The maximum level of turbulent kinetic energy is typically a few percent of the thermal energy.

For example, Fig. 2 shows simulation results for pressure profiles at two times after plasma formation in an inverse pinch. By t = 8 μs, the plasma has settled into a stable profile that closely matches the Kadomtsev $Q_0 = 1$ marginal state at large radius (indicated with heavy line). At smaller radius the value of Q_0 is less than 1.

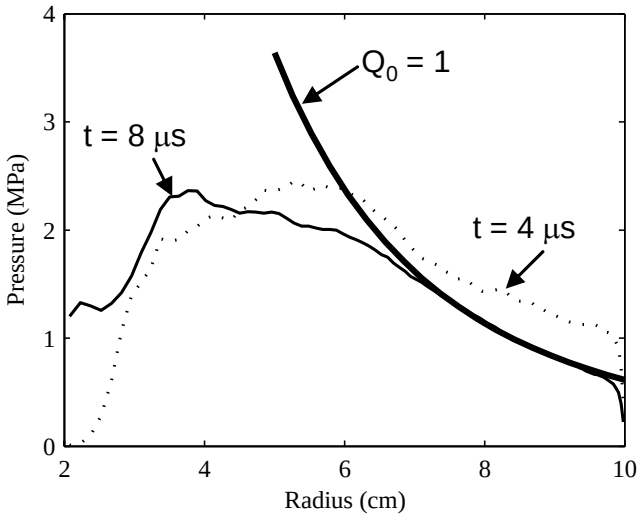

Also according to Kadomtsev, the stability of $m = 1$ requires separately that $Q_1 < 1$, where:

$$Q_1 = -\beta \frac{r}{p}\frac{dp}{dr} \qquad (2)$$

Comparison of Eqs. 1 and 2 shows that the $m = 1$ criterion is the one more stringent when β exceeds 2/5. Simulations suggest that β can be controlled during formation in an inverse pinch, and kept below 2/5 at all radial locations, by introducing a sufficient amount of initial bias magnetic field before plasma is formed. Typically the required bias current is about ¼ of the final level of applied current.

3. Compressional heating

The hard-core z pinch configuration suggests a liner compression approach in which the hard core remains stationary and the outer boundary implodes radially inward. A possible geometry is shown conceptually in Fig. 3. As the liner begins to implode, the region labeled "switch" in Fig. 3 causes the plasma injection gap to close. After that, plasma with flux is trapped in a toroidal chamber surrounding the hard core, and compressional heating occurs as the liner implodes. The liner shaping required for the switching action has not been examined in detail, but experience with shaped liners suggests that workable designs are possible [11].

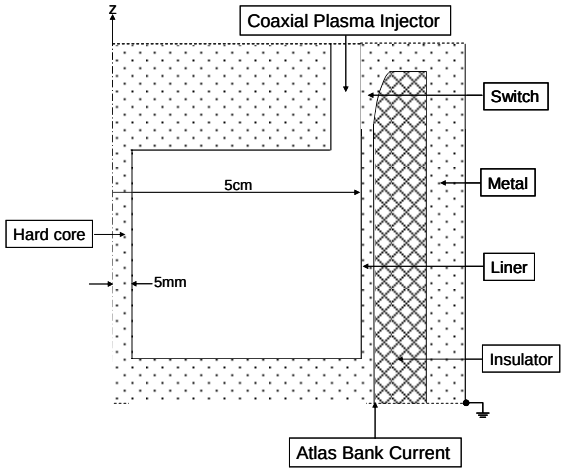

FIG. 3. Liner and diffuse z pinch geometry for implosion heating. Apparatus for injection of plasma connects electrically at the top. A liner implosion circuit such as Atlas connects at the bottom.

Compressional heating of a sub-kilovolt target plasma appears to be an effective way to achieve thermonuclear temperatures. For a preheated target the required implosion velocity can be less than the sound speed of the plasma, in contrast to ICF where carefully timed shocks are required to reach thermonuclear temperatures.

Heating is termed adiabatic if the implosion is slower than the magneto-sound velocity, but faster than heat transport or magnetic diffusion. The adiabatic limit, while not always applicable, is useful for understanding the physical process of heating, and often times for quasi-analytic approximations. However, even for the simple geometry of a diffuse z pinch, the analysis of adiabatic compression is somewhat complicated at high beta. The complications mostly arise because of the differences between effective $\gamma = 2$ for compression of magnetic field as opposed to $\gamma = 5/3$ for the plasma. Appendix A discusses analytically the adiabatic response of a diffuse z pinch during compression.

Using numerical methods the response of any intial plasma profile can be studied. Fig. 4 shows the adiabatic heating response assuming the pressure profile starts initially as a uniform-temperature Kadomtsev-marginal profile ($Q_0 = 1$ curve in Fig. 2) that extends from the hard core to the liner. Average temperature <T> is defined as total thermal energy U divided by 3N, where N is the (constant) number of ions in the chamber. Average beta <β> is defined as 2U/3Emag, where Emag is the total magnetic field energy in the chamber. Fig. 4 shows that starting with $A = 10$ (like that shown in Fig. 3), <T> in the adiabatic approximation can be increased by 10x (or 100x) as the aspect ratio is reduced to 1.4 (or 1.02). Average beta increases from 0.10 at first, reaches a maximum of 0.16 at $A = 1.6$, and then decreases.

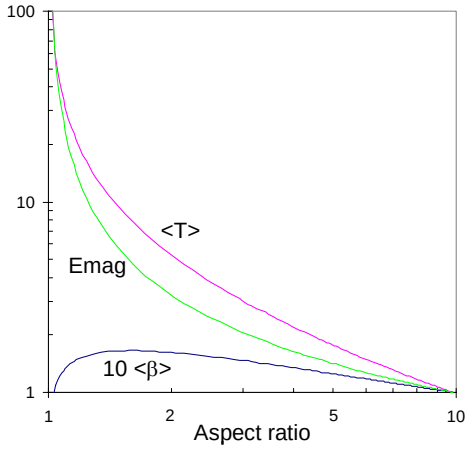

FIG. 4. Adiabatic compression increases temperature and magnetic field energy as aspect ratio decreases.

An important issue for compressional heating is what happens to stability during the process. To analyze $m = 0$ stability it is helpful to introduce a Kadomtsev parameter, $K = p^{3/5} r / B$, where the exponent of p is the reciprocal of the gas parameter. Given equilibrium as a constraint, the condition $\frac{\partial \mathrm{K}}{\partial r} > 0$ is then equivalent to $Q_0 < 1$. For the case of adiabatic compression, the pressure profile evolves in a way that conserves mass, flux and entropy. Therefore, an ideal plasma with no resistivity or heat losses conserves $\rho r / B$ and $p/\rho^{5/3}$ in each fluid element, and also the value of K. This means that if plasma elements do not change their relative radial positions, then for ideal isentropic motions they will stay in the same condition relative to $m = 0$ stability (stable, unstable, or marginal). In particular, if a plasma begins in the marginally stable state with $Q_0 = 1$ or equivalently K independent of r, then the value of Q_0 stays constant during compression.

Many aspects of the changing plasma β during compression, and the resulting influence on both $m = 1$ as well as $m = 0$ stability, can be understood by examining both numerical results and the analytic discussion of Appendix A. Qualitatively, one finds that the initial plasma equilibrium is distorted in a quite non-linear manner during compression. The value of β always decreases near the hard core during compression ($r/a \sim 1$), but it usually increases in regions of large r/a. There is a region where β remains nearly constant during large aspect ratio compression. Then as A approaches unity, β decreases at all radial locations.

The profile evolution obtained numerically is shown in Fig. 5 for the same Kadomtsev-stable profile of Q_0 = 1 used for Fig. 4. The initial maximum β at the inner wall is assumed to be 2/5, so at that location Q_1 is unity. At larger radii, β is smaller, so the value of Q_1 is smaller. Fig. 5 shows the values of Q_0 and Q_1 after compression as determined by taking numerical derivatives defined by Eqs. 1 and 2. For initial stages of compression with A larger than 2, the numerical value of Q_0 is very nearly constant, which is the expected result. The value of Q_0, is still close to unity for A = 1.2 as seen in Fig. 5, although a slight decrease of Q_0 appears as r/a approaches unity, and oscillations are seen as r/a approaches A. These departures from unity are numerical effect that arise because of the errors that occur when taking a numerical derivative. The numerical values of Q_1 become approximately uniform in radius and well below unity (away from the edge regions where numerical errors appear), which shows that the margin for stability to $m = 1$ is increased.

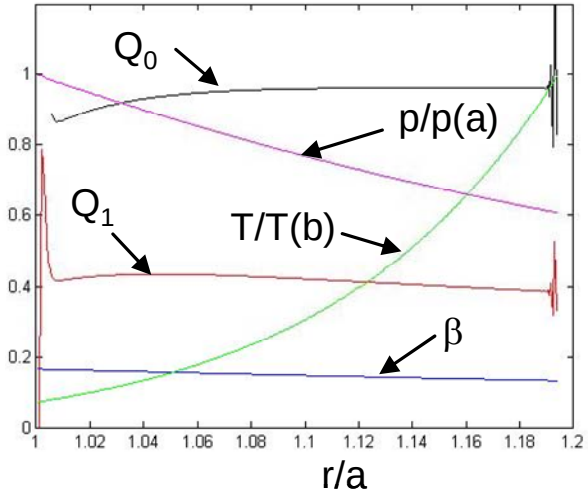

FIG. 5. Plasma pressure, temperature, beta, and Q profiles after adiabatic compression from A = 10 to A = 1.2.

To summarize, the previously described self-organization tends to generate $Q_0 < 1$. Adiabatic compression does not change Q_0, and reduces Q_1. Thus, from a stability perspective, compression of a diffuse z pinch appears to be a promising approach for heating.

4. Liner behavior during implosion.

For MTF, the relevant parameters for liner implosions are typically MA of current and MJ of energy. The Atlas facility, which is located at the DOE Nevada Test Site, is a good example of such a facility. Typical Atlas parameters are listed in Table 1. It was designed primarily for the purpose of imploding cylindrical liners to generate high pressures for studies of dynamic material properties, but the facility offers interesting potential as an MTF driver. The typical liner dimensions used in Atlas are similar to the sketch shown in Fig. 3.

TABLE 1. ATLAS PARAMETERS

Voltage	240 kV
Stored energy	24 MJ
Source inductance	~ 25 nH
Peak current	30 MA

A reasonable approximation for liner behavior during the early stages of implosion is to assume the liner material is an incompressible fluid. The motion can then be calculated using a zero-dimensional approximation [12]. At peak compression, Mbar pressures are generated. Then the liner and hard-core compressibility becomes important, and one source of inefficiency is the energy that goes into material compression. Another important effect is the eddy current heating of the liner and hard core surfaces. These effects can be quantified using a Los Alamos one-dimensional MHD code called RAVEN. The Lagrangian code uses material properties such as equation of state and resistivity obtained from the Los Alamos tabulated Sesame tables. Fig. 6 shows the expected behavior of a 10-cm long, 2-mm-thick aluminum liner driven by Atlas using the geometry of Fig. 3. The initial hard-core current is assumed to be 1.5 MA, and the space between the liner and the hard core is assumed to be a vacuum. The inner surface reaches a velocity of 3.3 km/s, and the liner KE reaches 650 KJ before deceleration begins. The implosion time is about 23 μs. The finite compressibility of aluminum can be seen by the displacement of the hard core surface at the time near peak compression. The magnetic field in the gap reaches a value of about 500 Tesla. The energy lost to compression effects is about 380 KJ or 42% of the kinetic energy.

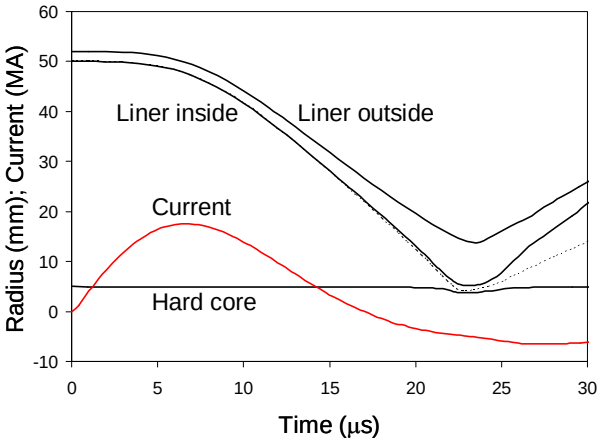

FIG. 6. Liner inner and outer radius, hard-core radius, and Atlas current vs. time assuming zero liner resistivity. Dotted line is inner liner radius with Sesame resistivity.

Eddy current heating during implosion causes the aluminum hard-core surface to boil just before the time of peak compression for the case presented in Fig. 6. Fig. 7 shows the temperature in eV near the hard-core surface for times near peak compression in the implosion. The liner inner surface boils slightly later in time because the larger radius has lower current density.

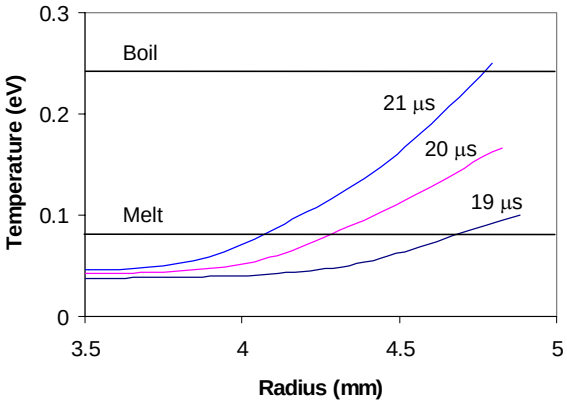

FIG. 7. Temperature (eV) vs. radius near surface of hard core at times near peak compression.

Because the space between the liner and the hard core is modeled as vacuum, flux diffuses at a rate determined by aluminum surface temperature and resistivity. The situation with a conducting plasma in the gap is different because the amount of flux that diffuses becomes limited by the plasma conductivity. The modeling reported here does not quantify this effect, but for reference, liner motion is computed either with perfect conductivity or realistic conductivity shown as a solid line or a dotted line respectively in Fig. 6. For the case with aluminum resistivity and vacuum conditions, the liner inner surface impacts directly upon the hard-core surface as seen by the dotted line.

5. Simulations of liner compression including plasma energy losses

It would be difficult in practice to implode as fast as required for strict application of the adiabatic approximation. Stable equilibrium of a hard-core diffuse z pinch requires plasma contact with metallic boundaries in both radial and axial directions. Thus heat losses and some degree of non-adiabatic behavior are expected. Taking into account thermal conduction and the Hall effect can destroy the Kadomtsev stable profiles and result in high convection fluxes. The convective effect near external metallic boundaries was analyzed and reported elsewhere [13]. Radiation losses are also expected to be important for plasma near the boundaries as wall impurities are swept into the chamber by plasma convection [14]. Efforts continue to be directed towards estimating and understanding these effects with increasingly realistic numerical simulations.

Results are presented here for Atlas-like parameters using the same two-dimensional MHD code previously used to explore self-organization. The compressible two-fluid model uses Braginskii coefficients of thermal conduction and electrical resistivity [7]. The assumed Ohm's law is $\boldsymbol{E}+\mathbf{v}\times\boldsymbol{B} = \eta\boldsymbol{j}$, which relates electric field **E**, fluid velocity **v**, magnetic field **B**, current **j**, and resistivity η. Thus the effects of compressional heating and cross-field thermal losses at cold boundaries enhanced by convective motion are included. Hall terms and thermoelectric terms such as the Nernst current are not included.

Simulation results are shown in Fig. 8. The numerical model uses as input a prescribed motion for the outer plasma boundary and assumes the inner boundary does not move. The outer boundary position is taken from the RAVEN calculations by assuming the gap between the inner liner surface and the hard core is the same as determined by RAVEN assuming zero resistivity (solid line in Fig. 6).

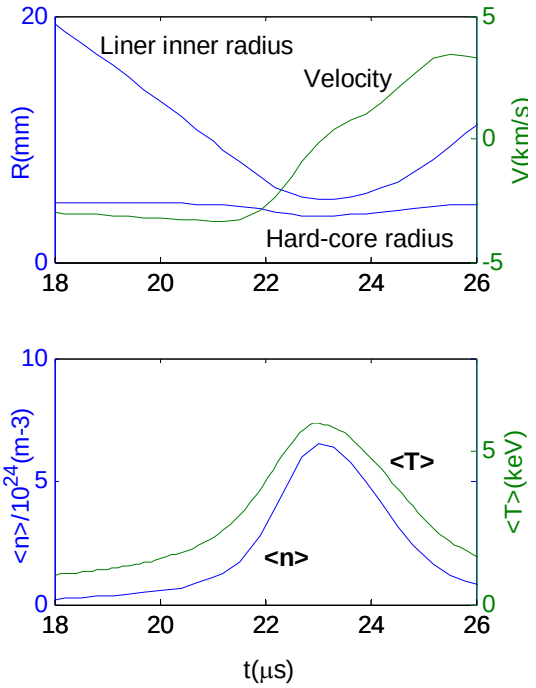

FIG. 8. Numerical simulation of plasma parameters during liner compression assuming prescribed boundary motion based on Atlas parameters.

The injection process is not modeled in the simulation reported here. The target plasma is assumed to have 30 KJ of energy generated with a 1.5 MA pulse of current before the liner implosion begins, which are reasonable parameters expected from coaxial accelerators. The temperature is assumed to be uniform at 500 eV, and the initial pressure profile is assumed to be a Kadomtsev-stable profile with Q_0=1 and $\langle\beta\rangle$ = 0.1 extending from the hard core to the liner as discussed above. The corresponding average ion density is 4 x10^{22} m^{-3}.

Fig. 8 shows the time dependent average temperature reaching 6 keV and average density of about 6x10^{24} m^{-3} at the time of peak compression. According to these results, a deuterium plasma would generate 4x10^{12} neutrons. Time-resolved neutrons should be detectable starting at about 20 μs based on previous experience with scintillator detectors. For comparison, a

strictly adiabatic calculation would give maximum average temperature of about 7 keV and $3x10^{13}$ neutrons. Note that the graph for liner velocity indicates that liner deceleration and Rayleigh-Taylor instabilities would not be expected until about 22 μs, well after neutron emission should begin. Thus, the time variation of neutron emission would give valuable information about the final stages of plasma compression.

6. Conclusions

The prospects for an interesting MTF liner implosion experiment have been examined based on the existing Atlas facility. Experience with MAGO and other types of coaxial accelerators give hope that a moderate-cost plasma injector with the needed properties could be developed. The stabilized hard-core z pinch appears to have interesting properties for MTF, and the geometry is well suited to the Atlas hardware.

7. Acknowledgements.

This work was sponsored at the University of Nevada, Reno by DOE OFES Grant DE-FG02-04ER54752, by DOE NNSA/NV Cooperative Agreement DE-FC08-01NV15050, and by DOE EPSCoR grant xxxxxxxxx.

This work was performed under the auspices of the U.S. Department of Energy by University of California, Lawrence Livermore National Laboratory under contract W-7405-Eng-48.

Appendix A. Adiabatic compression of a diffuse z pinch.

1. Introduction. We analyze here adiabatic compression of a diffuse z pinch by a radially imploding external shell (or liner) as indicated in Fig. A1. We assume the diffuse z pinch plasma has been established with a stable equilibrium as discussed in the text. We have in mind the stabilized hard-core situation, but much of the analysis applies as well to a diffuse z pinch without a hard core. Adiabatic refers to a slow implosion in the sense that the liner velocity is much smaller than the magneto-sound velocity, but fast in the sense that heat transport and magnetic diffusion are negligible. The magneto-sound velocity is equal to the sound speed at high betas, and to the Alfven speed at low betas. Both the central rod and the external shell are assumed to be perfect conductors. One of the interesting results of this analysis will be that plasma beta can increase or decrease during the implosion depending upon the amount of compression and which region of the plasma is under consideration.

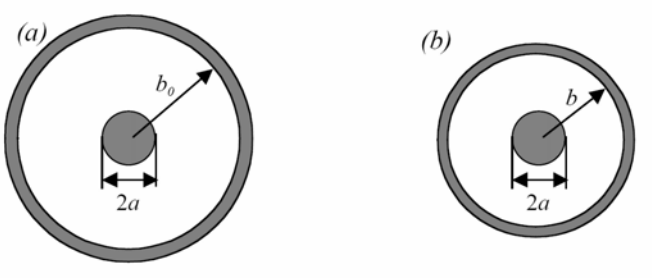

Fig. A1. A hard-core pinch configuration during the implosion of a conducting shell: (a)Initial state; the radius of the outer shell is b_0. (b) The state reached after the shell radius becomes $b<b_0$. We assume that the radius of the central rod does not change.

2. Basic equations. The slowness of the compression process allows us to consider the plasma evolution as a set of equilibria determined by the instantaneous value of the shell radius b. The magnetic field has only an azimuthal component, and the current has only an axial component in the diffuse z pinch. Therefore, at any instant of time the pressure profile and magnetic field as functions of radius are solutions to:

$$\frac{dp}{dr}+\frac{1}{2\mu_0 r^2}\frac{d}{dr}(rB)^2=0 \qquad \text{(A1)}$$

The Lagrangian description of this problem is useful. In the initial state, the plasma pressure, density, and magnetic field, are functions of the radius r_0 given by $p_0(r_0)$; $\rho_0(r_0)$; and $B_0(r_0)$. In the state where the external shell radius has become b, a flux surface whose initial radius was r_0 moves to some radius r:

$$r=r(r_0,b) \qquad \text{(A2)}$$

The value of b enters this equation as a parameter. Obviously, the function $r(r_0,b)$ satisfies the following relations:

$$a=r(a,b);\, b=r(b_0,b) \qquad \text{(A3)}$$

As a consequence of mass and flux conservation we have:

$$\rho=\rho_0(r_0)\left(\frac{r}{r_0}\frac{dr}{dr_0}\right)^{-1} \qquad \text{(A4)}$$

$$B=B_0(r_0)\left(\frac{dr}{dr_0}\right)^{-1} \qquad \text{(A5)}$$

Pressure follows the adiabatic relation:

$$p = p_0(r_0)\left(\frac{r}{r_0}\frac{dr}{dr_0}\right)^{-1} \qquad \text{(A6)}$$

Switching from differentiation over r to differentiation over r_0 in Eq. A1, we find the following equation which, together with the boundary conditions of Eq. A3 determines the function $r(r_0,b)$ for any given b:

$$\frac{d}{dr_0}\left[p_0(r_0)\left(\frac{r}{r_0}\frac{dr}{dr_0}\right)^{-\gamma}\right] + \frac{1}{2\mu_0 r^2}\frac{d}{dr_0}\left[(rB_0)^2\left(\frac{dr}{dr_0}\right)^{-2}\right] = 0 \qquad \text{(A7)}$$

After the function $r(r_0,b)$ is found, one then computes the pressure and the magnetic field in the new state by using Eqs. A5 and A6. The plasma beta in the new state is given as:

$$\beta = \beta_0(r_0)\left(\frac{r_0}{r}\right)^2\left(\frac{r}{r_0}\frac{dr}{dr_0}\right)^{2-\gamma} \qquad \text{(A8)}$$

Eq. A7 is a complex non-linear equation, which in general can be solved only numerically. We discuss here two limiting cases where a simple analytic solution is possible, the cases of high betas or low betas.

3. High-beta plasma (wall confinement). In the case of high-beta which can occur with wall confinement, the second term in Eq. A7 can be neglected. This amounts to a zero-order approximation in the parameter $1/\beta$; higher-order corrections can also be derived easily. The initial plasma pressure in zero order is then just uniform pressure $p_0(r_0)$=constant. Eq. A7 gives:

$$\frac{r}{r_0}\frac{dr}{dr_0} = C_1, \qquad \text{(A9)}$$

and

$$r^2 = C_1 r_0^{\,2} + C_2, \qquad \text{(A10)}$$

The integration constants C1 and C2 can be found from the boundary conditions in Eqs. A3, which gives the result:

$$r^2 = \frac{\left(b^2 - a^2\right)r_0^{\,2} + a^2\left(b_0^{\,2} - b^2\right)^2}{b_0^{\,2} - a^2}, \qquad \text{(A11)}$$

The plasma beta is determined by substituting Eq. A11 into Eq. A8:

$$\beta = \beta_0(r_0)\frac{\left(b_0^{\,2} - a^2\right)r_0^{\,2}}{\left(b^2 - a^2\right)r_0^{\,2} + a^2\left(b_0^{\,2} - b^2\right)}\left(\frac{b^2 - a^2}{b_0^{\,2} - a^2}\right)^{1/3} \qquad \text{(A12)}$$

Here the numerical value of γ is used for a fully ionized plasma (γ=5/3).

For the diffuse pinch with a=0, we have:

$$\beta / \beta_0(r_0) = \left(\frac{b_0}{b}\right)^{4/3} > 1, \qquad \text{(A13)}$$

so, one concludes that beta everywhere increases during adiabatic compression in a diffuse high-beta z pinch as noted previously in Ref. 3.

For the hard-core z pinch the situation is more complex. The beta can increase or decrease depending upon the position r_0 and on the aspect ratio $A=b/a$. We also use the notation $A_0 = b_0/a$. Near the central rod, beta universally decreases. We see that by putting $r_0 = a$, and finding from Eq. A12 that:

$$\beta / \beta_0(a) = \left(\frac{b^2 - a^2}{b_0^{\,2} - a^2} \right)^{1/3} < 1, \qquad \text{(A14)}$$

This happens because the compression occurs in an almost planar fashion next to the hard core. On the other hand, for a large-enough A, compression in the outer parts of the pinch occurs essentially in the same way as in a diffuse pinch, and beta increases. To see that we examine Eq. A12 for $r_0 = b$, and find:

$$\beta / \beta_0(b) = \left(\frac{b_0^{\,2}}{b^2} \right) \left(\frac{b^2 - a^2}{b_0^{\,2} - a^2} \right)^{1/3}, \qquad \text{(A15)}$$

From Eq. A12 one can show that for $b_0/a > (3/2)^{1/2}$, the beta at the plasma periphery increases with decreasing b, until b/a becomes equal to $(3/2)^{1/2}$. After that it decreases and eventually reaches the initial value at the aspect ratio determined by the equation:

$$A^2 = \frac{A_0^{\,2}}{2} \left(\sqrt{1 + \frac{4}{A_0^{\,2} - 1}} - 1 \right), \quad A_0 > \sqrt{3/2} \qquad \text{(A16)}$$

With further compression beta becomes smaller than its initial value at all radii.

If the condition $A_0 > (3/2)^{1/2}$ holds, and A is greater than the value determined by Eq. A16, there exists an inversion radius r_0^* that separates the outer region where β/β_0 increases during compression ($r_0 > r_0^*$) and an inner region where β/β_0 decreases ($r_0 < r_0^*$). The dependence of r_0^* vs. A for $A_0 = 3$ is shown in Fig. A2.

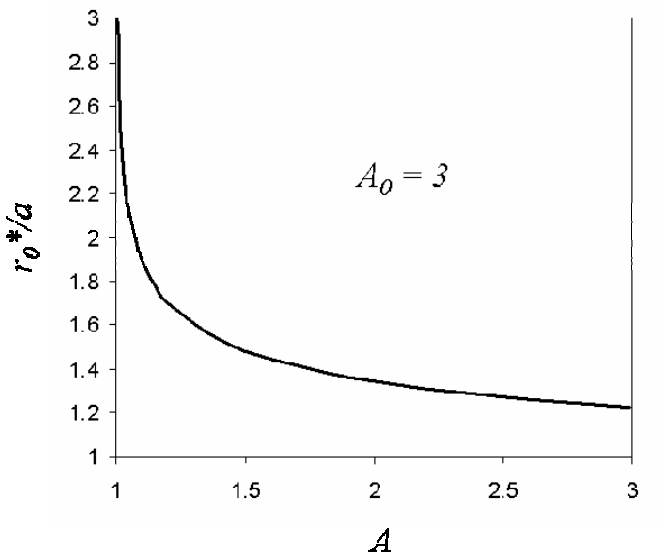

Fig. A2. The inversion radius for high-beta plasma, outside of which β grows larger than its initial value during compression to aspect ratio A = b/a, and inside of which β grows smaller. For this example, the initial value b_0/a is taken as aspect ratio $A_0 = 3$.

We see in Fig. 2A that as the liner approaches the hard core radius, or equivalently, as A approaches unity, r_0^*/a approaches A_0 This means that plasma at all initial locations has reduced beta after compression. Conversely, for

moderate compression to say $A = 2$, plasma located initially with r_0 greater than about 1.4 a has increasing beta.

For the high-beta compression under consideration, Fig. A3 shows the ratio of the final beta to initial beta *vs*. the initial plasma location r_0 for various values of aspect ratio A, assuming $A_0 = 3$.

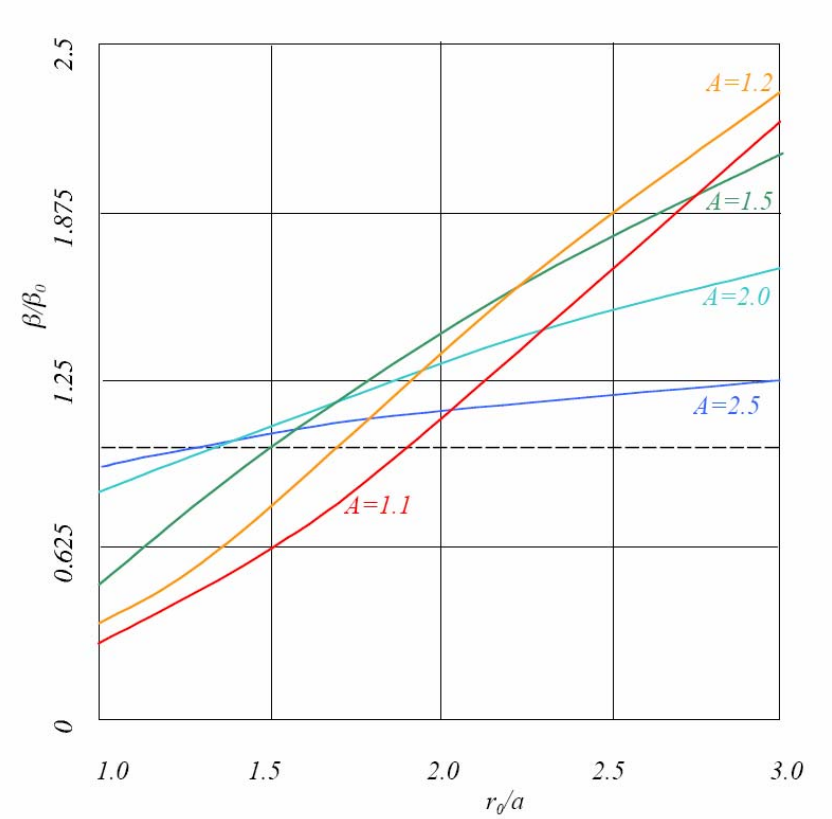

Fig. A3. Final beta relative to initial beta for high-beta plasma as a function of initial plasma location. Numerical example is presented assuming initial aspect ratio is $A_0 = 3$, the same as in Fig. A2.

The tendency by which more and more plasma has reduced beta as compression increases, which was mentioned above in connection with Fig. A2, can also be seen in Fig. A3. The location of r_0/a where β/β_0 equals unity increases monotonically as A increases.

4. Low-beta plasma. In the configuration being considered, the low-beta case is possible only in the presence of a central post. Without the central post, the local value of beta becomes infinite at the axis where B must be zero by symmetry. For a low-beta solution, the plasma currents must be small compared to the current in the central post. In this case, one can neglect the first term in Eq. A6. Also, B_0 in this case is proportional to $1/r_0$. We then can say:

$$\frac{dr}{dr_0} = D\frac{r}{r_0}, \qquad \text{(A17)}$$

where D is an arbitrary constant. Accordingly, using the first of the boundary conditions Eq. A3, one finds:

$$\ln\frac{r}{a} = D\ln\frac{r_0}{a}, \qquad \text{(A18)}$$

Applying the second of the boundary conditions A3, one obtains:

$$\ln\frac{r}{a} = \left(\frac{\ln\frac{b}{a}}{\ln\frac{b_0}{a}}\right)\ln\frac{r_0}{a}, \tag{A19}$$

and

$$\frac{dr}{dr_0} = \left(\frac{\ln\frac{b}{a}}{\ln\frac{b_0}{a}}\right)\frac{r}{r_0} \tag{A20}$$

Substituting this result into Eq. A8, one gets:

$$\beta / \beta_0(r_0) = \left(\frac{r}{r_0}\right)^2 \left(\frac{\ln\frac{b}{a}}{\ln\frac{b_0}{a}}\right)^{2-\gamma} \tag{A21}$$

Because $r < r_o$, and $b < b_0$, the beta in this case universally decreases.

REFERENCES

[1] V. Makhin *et al*., to be published, Phys. of Plasmas (2005).
[2] D. D. Ryutov *et al*., Nuc. Fusion **43**, 955 (2003).
[3] R. P. Drake, J. Hammer, C. W. Hartman, L. J. Perkins, D. D. Ryutov, Fusion Technology **30**, 310 (1996).
[4] I. R. Lindemuth, *et al*., Phys. Rev. Letts. **75**, 1953 (1995).
[5] I. R. Lindemuth, *et al*., *"Magnetic Compression / Magnetized Target Fusion (MAGO/MTF): A Marriage of Inertial and Magnetic Confinement*, 16th IAEA Fusion Energy Conference, Montreal, Canada, October 7-11, 1996.
[6] B. S. Bauer *et al*., Bull. Am. Phys. Soc. **48**, CP1-24 (2003).
[7] A. Esaulov *et al*., Phys. of Plasmas **11**, 1589 (2004).
[8] A. M. Buyko *et al*, Pulsed Power Plasma Science 2001 Conference, Las Vegas, Nevada, USA, p.516, June 17-22, 2001.
[9] R. E. Reinovsky, W. L. Atchison, R. J. Faehl, I. R. Lindemuth, Proc. 14th IEEE International Pulsed Power Conference, p. 94, Dallas, Texas, USA, June 15-18, 2003.
[10] B. B. Kadomtsev, *Reviews of Plasma Physics*, edited by M.A. Leontovich (Consultants Bureau, New York), Vol. **2**, 153 (1966).
[11] J. H. Degnan *et al*., *Deformable Contact Liner Implosion Performed with 8 cm Diameter Electrode*, Proc. 2004 IEEE International Conference on Plasma Science, p.161, Baltimore, MD, USA, June 28-July 1, 2004.
[12] T. Goodrich, *et al*., Bull. Am. Phys. Soc. **49**, (2004).
[13] S. F. Garanin, G. G. Ivanova, V. I. Mamyshev, V. N. Sofronov, *Convective cooling of plasma during its 2D turbulent flow in magnetic field*, Paper C-25, The X-th International Conference on Megagauss Magnetic Field Generation and related Topics, Berlin, Germany, July 18-23, 2004.
[14] S. F. Garanin, V. I. Mamyshev, E. M. Palagina, *Wall material washout by plasma during its 2D flow in magnetic field*, Paper C-57, The X-th International Conference on Megagauss Magnetic Field Generation and related Topics, Berlin, Germany, July 18-23, 2004.